CYBERNETICS AND PHYSICS, VOL. 13, NO. 1, 2024, 69–76

COMBINED REPETITIVE CONTROL SYSTEM FOR ACTIVE DAMPING OF FORCED VIBRATIONS

Evgeniy Shelenok
Higher School of Cybernetics and Digital Technologies
Pacific National University
Russia
cidshell@mail.ru

Article history:
Received 07.05.2024, Accepted 09.06.2024

Abstract

The consideration was given to the damping of periodic vibrations acting on vibration protected plant using a hydraulic support with active control. A nonlinear robust-adaptive repetitive control system was synthesized for the technical plant under consideration. The author uses a piezoelectric accelerometer to measure acting vibrations, the generator for periodic signals to compensate for repetitive force action and the hyperstability criterion to synthesize a control algorithm. In the final section it was present a computational experiment whose results clearly illustrate the quality of the obtained control system.

Key words

Vibration damping, active hydraulic support, measurements, accelerometer, hypertability criterion, repetitive control system.

1 Introduction

The problems of compensating for external disturbances that affect the operation processes of various technical plans are among the relevant issues of modern automatic control theory and practice [Bui and Margun, 2022; Nguyen et al., 2022; Tsykunov, 2010; Furtat, 2013; Quoc et al., 2021; Izrailovich and Grishaev, 2012; Andrievsky and Furtat, 2020a; Andrievsky and Furtat, 2020b]. Reducing unwanted vibrations in machines and mechanisms is an important application associated with solving such problems. In this context, the main priority is to develop methods for damping external repetitive disturbances that result from kinematic or force effects on the vibration protected plant, which cause an increase in the intensity of its forced vibrations.

To measure external vibrations, it is necessary to use various measuring transducers (sensors), whose quality characteristics directly affect the system's performance. Nowadays, there is a wide range of measuring devices available that can measure vibration displacements across a broad spectrum of frequencies and amplitudes with varying degrees of accuracy. The choice of sensors primarily depends on the specific problem being solved. Both optical and piezoelectric sensors are widely used for constructing vibration damping and control systems.

Optical sensors have proven effective for measuring both fairly large oscillations with an amplitude of 0.5 mm (optical wedges) and small amplitudes of several micrometers (interferometers and lasers). The main advantages of these sensors are the absence of inertia and simplicity of design. However, the use of optical converters requires an additional power source and, in some cases, a photocell, which may not always be feasible to install.

These disadvantages are absent in accelerometers, which are built using the piezoelectric effect in crystals, ceramics or films and convert mechanical energy into electrical [Johnson et al., 1980]. In particular, they generate an electrical signal that is proportional to the acceleration of the measured vibrations. These sensors do not require an auxiliary power supply, possess a simple design, linear characteristics, wide dynamic operating ranges, and high operational reliability. Unlike optical sensors, accelerometers have an inertia, which must be considered when developing algorithms for control devices. Piezoelectric sensors find extensive application in the construction of various vibration control systems.

In most practical cases developers use active vibration damping systems to reduce external cyclic loads. These systems generate control signals that are calculated using feedback and applied to one or several parts of the protection plant. An example of such a control system is a hydraulic vibration support with active control

[Izrailovich and Grishaev, 2012]. The known to-date results have made it possible to improve the quality of vibration protection systems of the indicated class. But the problem of constructing universal control laws that guarantee high quality for plants with previously unknown parameters remains open.

From the perspective of control theory, the problem of reducing for unwanted vibrations should be considered as a problem of stabilization of a priori uncertain plants relative to a certain balance position [Bui and Margun, 2022; Nguyen et al., 2022; Eremin and Shelenok, 2011]. At the same time, methods of adaptive and robust control are most advisable for designing feedback loop algorithms. [Bui and Margun, 2022; Nguyen et al., 2022; Eremin and Shelenok, 2011; Eremin et al., 2021; Pikina and Pashchenko, 2021]. Using these approaches, it is possible to develop algorithms that ensure sufficiently good control system performance within a fairly wide range of uncertainty in the controlled plant. At the same time, a notable method for developing control systems for uncertain plants is the hyperstability criterion proposed by V. M. Popov [Popov, 1973].

The construction of control loops based on the hyperstability criterion requires special approaches for plants whose mathematical models have a relative degree greater than one. One such method is including a high-speed correction filter in the main system's loop. This method allows us to develop control systems with a relatively simple structure for non-strictly minimal phase dynamic plants for fulfilling the special *L*-dissipativity conditions [Eremin and Shelenok, 2023; Shelenok, 2023; Eremin et al., 2022].

The article discusses the construction of a system for damping forced vibrations in a vibration protected plant using a hydraulic support, for which a combined adaptive-robust controller is synthesized. The solution methods involve the hyperstability criterion and *L*-dissipativity conditions. A direct-conversion micromechanical accelerometer is used for measuring vibration displacements.

2 Preliminaries

Let us consider the general structure of a vibration damping system with active hydraulic support depicted in Fig. 1 [Izrailovich and Grishaev, 2012].

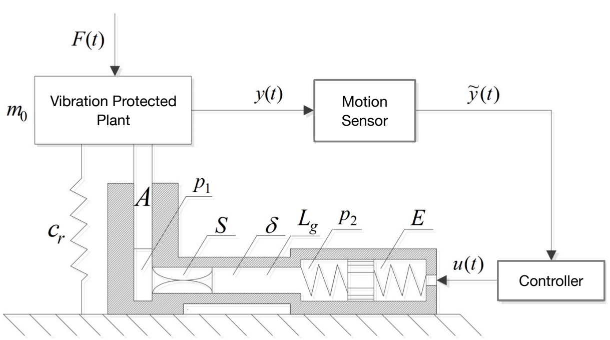

Figure 1. Scheme of the hydraulic support control system.

The mathematical model of this vibration support system is described using the following equations:

$$m_0\frac{d^2y(t)}{dt^2} + c_r y(t) = F(t) - Ap_1(t),$$
$$p_1(t) - p_2(t) = A\left(L\frac{d^2y(t)}{dt^2} + \delta\frac{dy(t)}{dt}\right),$$
$$Ep_2(t) - Ay(t) = \frac{E}{S}u(t).$$

where m_0 is the mass of the protected plant; A is the piston area; c_r is the stiffness of the passive damping element; $p_1(t)$ is the pressure in main hydraulic chamber ; δ is the linear hydraulic resistance; S is the membrane cross-sectional area; L_g is the hydraulic inertia; $p_2(t)$ is the pressure in additional hydraulic chamber; E is the capacity of the additional hydraulic chamber; $F(t) = B\sin(\varphi t)$ is an external periodic force disturbance, $B, \varphi = const > 0$; $y(t)$ represents the displacement of the protection plant; $\tilde{y}(t)$ represents the measured vibrations; $u(t)$ represents the control action applied to the additional hydraulic chamber.

Let us express $p_2(t)$ using the last equation provided:

$$p_2(t) = \frac{A}{E}y(t) + \frac{1}{S}u(t).$$

Next, we can define p_1 by substituting the resulting expression into the second equation:

$$p_1(t) = L_gA\frac{d^2y(t)}{dt^2} + \delta A\frac{dy(t)}{dt} + \frac{A}{E}y(t).$$

Thus, we describe the dynamics of the active hydraulic support as follows:

$$\left(m_0 + L_gA^2\right)\frac{d^2y(t)}{dt_2} + \delta A^2\frac{dy(t)}{dt} + \\ + \left(c_r + \frac{A^2}{E}\right)y(t) = F(t) - \frac{A}{S}u(t), \quad (1)$$

It is possible to represent model (1) as follows:

$$W_{HS}(s) = \frac{y(s)}{\overline{u}(s)} = \frac{1}{\overline{a}_1s^2 + \overline{a}_2s + \overline{a}_3}, \quad (2)$$

where $W_{HS}(s)$ represents the transfer function of hydraulic support; s is the complex variable; $y(s)$ and $\overline{u}(s)$ are the Laplace transforms of the output signal $y(t)$ and input signal $u(t)$, respectively;

$$\overline{u}(t) = F(t) + \overline{b}u(t),\ \overline{b} = -\frac{A}{S},$$
$$\overline{a}_1 = m_0 + L_gA^2,\ \overline{a}_2 = \delta A^2, \overline{a}_3 = \left(c_r + \frac{A^2}{E}\right). \quad (3)$$

We connect a direct-conversion micromechanical accelerometer to the output of the protection plant to measure its movement amplitude. It is well known [Johnson et al., 1980] that model of this sensor can be represented as a series connection of the transfer function for a sensing element, the transfer function for a displacement transducer, and the transfer function for a low-pass filter [Johnson et al., 1980]:

$$W_{MA}(s) = \frac{U_{out}(s)}{y(s)} = \\ = \frac{mU_{rv}K_yK_f}{h_0(T_y^2s^2+2\zeta_yT_ys+1)(T_f^2s^2+2\zeta_fT_fs+1)}, \quad (4)$$

where $U_{out}(s)$ represents the Laplace transform of the sensor output $U_{out}(t)$; m is the mass of the sensing element; U_{rv} is the internal reference voltage; K_y is the sensing element gain; K_f is the low-pass filter gain; h_0 is the gap between movable and stationary parts of the sensor; $T_y = \sqrt{m/G_y}$ is the time constant of the sensing element; G_y is the linear rigidity of the sensing element suspension; ζ_y is the damping coefficient for oscillations of the sensitive element; T_f i is the time constant of the low-pass filter; ζ_f is the damping coefficient for oscillations of the low-pass filter.

A generalizes transfer function for the control plant (*CP*) can be represented as follows:

$$\begin{gathered} W_{CP}(s) = W_{HS}(s)W_{MA}(s) = \\ \frac{U_{out}(s)}{\overline{u}(s)} = \frac{\alpha(s)}{\beta(s)}, \alpha(s) = K, \\ \beta(s) = h_0\left(\overline{a}_1s^2+\overline{a}_2s+\overline{a}_3\right)\times \\ \times(T_y^2s^2+2\zeta_yT_ys+1)(T_f^2s^2+2\zeta_fT_fs+1), \end{gathered} \quad (5)$$

where $K = mU_{rv}K_yK_f$; $\beta(s)$ is the polynomial with an arbitrary roots.

Since the degree of transfer function (5) is $\rho = = \deg\beta(s) - \deg\alpha(s) = 6$ to construct an operable system, we connect a fast-acting dynamic correction filter (*DCF*) to the output of (5), similarly to [Eremin and Shelenok, 2023; Eremin et al., 2022], with the following description

$$W_{DCF}(s) = \frac{y_{ml}(s)}{U_{out}(s)} = \frac{\delta(s)}{\gamma(s)} = \left(\frac{Ts+1}{T_0s+1}\right)^5, \quad (6)$$

where $y_{ml}(s)$ represents the Laplace transform of the system's main loop output signal $y_{ml}(t)$; $\delta(s)$ and $\gamma(s)$ are Hurwitz polynomials; T and T_0 are time constants; T_0 is sufficiently small.

The serial connection of (5) and (6) has the following form:

$$\begin{gathered} y_{ml}(s) = W_{CP}(s)W_{DCF}(s)\overline{u}(s) = \\ = K\frac{1}{\beta(s)}\cdot\frac{\delta(s)}{\gamma(s)}\overline{u}(s) = K\frac{\delta(s)}{\beta(s)}\cdot\frac{1}{\gamma(s)}\overline{u}(s). \end{gathered}$$

In this case if we set a small value for the time constant $T_0 \ll 1$, then there will be a fair relation

$$\frac{1}{\gamma(s)} = \frac{1}{(T_0s+1)^5} \cong 1.$$

Consequently, we can replace the *actual connection* model of *CP* and *DCF* with the following approximate model

$$y_{ml}(s) \cong \frac{K\delta(s)}{\beta(s)}\overline{u}(s). \quad (7)$$

The mathematical model of this system, incorporating equations (1)-(5) and (7) in state-space form, is described as follows:

$$\begin{gathered} \frac{d\mathbf{x}(t)}{dt} = \mathbf{A}\mathbf{x}(t) + \mathbf{b}\tilde{b}u(t) + \mathbf{f}(t), \\ y_{ml}(t) = \mathbf{g}^T\mathbf{x}(t),\ \mathbf{x}(0) = \mathbf{x}_0, \end{gathered} \quad (8)$$

where $\mathbf{x}(t) \in \mathbf{R}^6$ is the state vector; $\mathbf{x}_0$ represent the vector of initial conditions; $\mathbf{A}$, $\mathbf{b}$ and $\mathbf{f}(t)$ are state matrix, control and external perturbations vector, respectively, having following structure:

$$\mathbf{A} = \begin{pmatrix} 0 & 1 & 0 & 0 & 0 & 0 \\ 0 & 0 & 1 & 0 & 0 & 0 \\ 0 & 0 & 0 & 1 & 0 & 0 \\ 0 & 0 & 0 & 0 & 1 & 0 \\ 0 & 0 & 0 & 0 & 0 & 1 \\ \beta_1 & \beta_2 & \beta_3 & \beta_4 & \beta_5 & \beta_6 \end{pmatrix},\ \mathbf{b} = \begin{pmatrix} 0 \\ 0 \\ 0 \\ 0 \\ 0 \\ \tilde{b} \end{pmatrix}, \quad (9)$$
$$\mathbf{f}^T(t) = \begin{pmatrix} 0 & 0 & 0 & 0 & 0 & f_6(t) \end{pmatrix},$$

$$\begin{gathered} \beta_1 = \frac{a_7}{a_1},\ \beta_2 = \frac{a_6}{a_1},\ \beta_3 = \frac{a_5}{a_1},\ \beta_4 = \frac{a_4}{a_1}, \\ \beta_5 = \frac{a_3}{a_1},\ \beta_6 = \frac{a_2}{a_1},\ \tilde{b} = K\overline{b}, \end{gathered}$$

$$\begin{gathered} a_1 = \overline{a}_1h_0T_y^2T_f^2, \\ a_2 = h_0\left\{T_yT_f\left[2\overline{a}_1\left(T_y\zeta_f+T_f\zeta_y\right)+\overline{a}_2\right]\right\}, \\ a_3 = h_0\{\overline{a}_1\left[T_y^2+4T_yT_f\zeta_y\zeta_f+T_F^2\right]+ \\ +T_yT_f\left[2\overline{a}_2\left(T_y\zeta_f+T_f\zeta_y\right)+\overline{a}_3T_yT_f\right]\}, \\ a_4 = h_0[2\overline{a}_1\left(T_y\zeta_y+T_F\zeta_f\right)+\overline{a}_2(T_y^2+4T_yT_f\zeta_y\zeta_f+ \\ +T_f^2)+2\overline{a}_3T_yT_f\left(T_y\zeta_f+T_f\zeta_y\right)], \\ a_5 = h_0[\overline{a}_1+2\overline{a}_2\left(T_y\zeta_y+T_f\zeta_f\right)+ \\ +\overline{a}_3\left(T_y^2+4T_yT_f\zeta_y\zeta_fT_f^2\right)], \\ a_6 = h_0\left[\overline{a}_2+2\overline{a}_3\left(T_y\zeta_y+T_f\zeta_f\right)\right],\ a_7 = h_0\overline{a}_3, \\ f_6(t) = KF(t). \end{gathered}$$

We determine the coefficients of a time-invariant vector $\mathbf{g}^T = \begin{pmatrix} g_1 & g_2 & g_3 & g_4 & g_5 & g_6 \end{pmatrix}$ which forms the output signal

$y_{ml}(t)$ from the following relations

$$g(s) = g_6 s^5 + g_5 s^4 + g_4 s^3 + g_3 s^2 + \\ + g_2 s + g_1 = \frac{\delta(s)}{a_1} = \frac{(Ts+1)^5}{a_1}, \\ g_1 = \frac{1}{a_1},\ g_2 = \frac{5T}{a_1},\ g_3 = \frac{10T^2}{a_1},\ g_4 = \frac{10T^3}{a_1}, \\ g_5 = \frac{5T^4}{a_1},\ g_6 = \frac{T^5}{a_1}. \tag{10}$$

We describe a priori uncertainty conditions for the considered model (8) – (10) as follows:

$$\mathbf{A} = \mathbf{A}(\boldsymbol{\xi}),\ \mathbf{b} = \mathbf{b}(\boldsymbol{\xi}),\ \mathbf{g} = \mathbf{g}(\boldsymbol{\xi}),\ \mathbf{f} = \mathbf{f}_{\boldsymbol{\xi}}(t), \tag{11}$$

where $\boldsymbol{\xi}^T = \left(m\ m_0\ U_{rv}\ K_y\ K_f\ T_y\ T_f\ \zeta_y\ \zeta_f\ h_0\right)$ is the vector of unknown parameters whose values belong to the known bounded numerical setΞ.

3 Problem Statement

Let us generate the required trajectory for the *CP*'s output $y(t)$ with a command signal $r(t)$ (tracking mode). If we aim to maintain the balance of *CP*, then command signal will be $r(t) = r^* = const \geq 0$ (stabilization mode). We will use the dynamic unit (command correction filter, *CCF*), equivalent to the *DCF* model, to set the required dynamics of the main control loop

$$\tilde{r}(s) = W_{DCF}(s) r(s) = \left(\frac{Ts+1}{T_0 s+1}\right)^5 r(s), \tag{12}$$

where $\tilde{r}$ represents the Laplace transform of some additional command signal $r(t)$ (output of the *CCF*).

The two control goals need to be formulated.

1. *Main control goal*: it is necessary to ensure the high-precision processing of the reference signal $r(t)$. This requirement entails achieving the following condition:

$$\lim_{t\to\infty} |r(t) - y(t)| \leq \Delta,\ \Delta = const > 0; \tag{13}$$

2. *Auxiliary control goal*: it is necessary to synthesize an explicit form of the control law $u(t) = = u(y_{ml}(t), r(t))$ that ensures the fulfillment of the following inequality

$$\lim_{t\to\infty} |y^*(t) - y_{ml}(t)| \cong \\ \cong \lim_{t\to\infty} |\tilde{r}(t) - y_{ml}(t)| \leq \Delta_{ml}, \\ \Delta_{ml} = const > 0, \tag{14}$$

for any initial conditions $\mathbf{x}_0$, bounded disturbances $|F(t)| \leq F_0,\ F_0 = const > 0$ and under a given level of uncertainty $\xi \in \Xi$.

In equations (13) and (14): Δ is a small constant corresponding to the specified tracking accuracy (for *CP*); Δ_{ml} is a small value corresponding to the maximum permissible tracking error (for a system's main control loop); $y^*(t)$ represents an output signal of the implicit reference model [Eremin et al., 2021]

$$y^*(t) = \frac{1}{\chi^{-1}p+1}\tilde{r}(t) = \frac{\chi}{p+\chi}\tilde{r}(t), \tag{15}$$

$p = d/dt$; $\chi = const > 0$. In addition, for $\chi \gg 0$ model (15) can be represented as:

$$y^*(t) \cong \tilde{r}(t). \tag{16}$$

Thus, if we ensure the auxiliary objective (14) through the synthesis of feedback algorithms, then the main control goal (13) will be achieved in the control system.

4 Main Results

We need to make one important remark before the synthesis procedure begins. When we consider a serial connection of *CP* and *DCF* (7), we will use an analogue of the reference model (15), which has the following equivalent form:

$$y^*(t) = \frac{\chi g(p) g_6}{(p+\chi)\, g(p) g_6}\tilde{r}(t) = \\ = \frac{\hat{\chi} g(p) g_6}{(p+\chi)\, g(p)}\tilde{r}(t),\ \ \hat{\chi} = \chi g_6^{-1}. \tag{17}$$

The reference model (17) can be represented in the following state-space form:

$$\frac{d\mathbf{x}^*(t)}{dt} = \mathbf{A}_*\mathbf{x}^*(t) + \mathbf{b}\hat{\chi}\tilde{r}(t), \\ y^*(t) = \mathbf{g}^T\mathbf{x}^*(t),\ \ \mathbf{x}^*(0) = 0, \tag{18}$$

where $\mathbf{x}^*(t) \in \mathbf{R}^6$ is the reference state vector, and $\mathbf{A}_* = \mathbf{A} - \mathbf{b}\chi\mathbf{g}^T$ is the Hurwitz matrix of the appropriate size.

Let us consider the deviation between the reference states and the internal states of the modified plant (7): $\mathbf{e}(t) = \mathbf{x}^*(t) - \mathbf{x}(t)$. In this case, with respect to (18) and (8), we can write down a description of the equivalent system's model as follows:

$$\frac{d\mathbf{e}(t)}{dt} = \mathbf{A}_*\mathbf{e}(t) + \mathbf{b}\mu(t),\ v(t) = \mathbf{g}^T\mathbf{e}(t) = \\ = y^*(t) - y_{ml}(t) \cong \tilde{r}(t) - y_{ml}(t), \\ \mu(t) = \hat{\chi}\tilde{r}(t) - \chi y_{ml}(t) - \tilde{b}u(t) - f_6(t), \tag{19}$$

where $\mu(t)$ represents a modified control signal; $v(t)$ represents a modified output signal.

We will satisfy the requirements of the hyperstability criterion, which involves resolving two positivity problems. In other words, we must provide conditions that guarantee the validity of two relations:

1. The frequency inequality for the linear time-invariant part (*LSP*) of the system (19)
$$\mathbf{Re}\left[\mathbf{g}^T\left(j\omega\mathbf{E}-\mathbf{A}_*\right)^{-1}\mathbf{b}\right]>0,\ \forall\omega\geq 0, \quad (20)$$
where $\mathbf{E}$ is the identity matrix of appropriate size;
2. The integral inequality for the nonlinear non-stationary part (*NNP*) of (19).
$$\eta(0,t)=-\int_0^t\mu(\varsigma)v(\varsigma)d\varsigma\geq-\eta_0^2, \quad (21)$$
$$\eta_0^2=const,\ \forall t>0.$$

IIn the present case, the transfer function of the system's *LSP* (19) coincides with the description of a first-order aperiodic link $W(s)=\mathbf{g}^T\left(s\mathbf{E}-\mathbf{A}_*\right)^{-1}\mathbf{b}=\dfrac{1}{\chi^{-1}s+1}$, for which condition (20) always holds. Therefore, we need to determine conditions (by synthesizing an explicit form of controller) that will ensure the inequality (21) holds

To achieve this, we represent the control signal as $u(t)=u_1(t)+u_2(t)$. Taking into account a signal $\mu(t)$ from (19), we can write down a left-hand side of the integral inequality (21) as follows:
$$\eta(0,t)=\tilde{b}\int_0^t\left(u_1(\varsigma)-\theta(\varsigma)\right)v(\varsigma)d\varsigma+$$
$$+\int_0^t\left(\tilde{b}u_2(\varsigma)+\chi y_{ml}(\varsigma)\right)v(\varsigma)d\varsigma= \quad (22)$$
$$=\sum_{i=1}^2\eta_i(0,t),$$
where $\theta(t)=\tilde{b}^{-1}\left(\hat{\chi}\tilde{r}(t)+f_6(t)\right)$ represents a periodic signal.

We define the explicit form of $u_1(t)$ as follows:
$$u_1(t)=u_1(t-\overline{T})+\gamma_1v(t),\ \ u_1(h)=0, \quad (23)$$
$$h\in\left[-\overline{T};0\right],\ \ \overline{T},\gamma_1=const>0.$$
Then for the first term in (22), we can obtain the following estimate [Eremin, 2003]:
$$\eta_1(0,t)=\gamma_1\tilde{b}\int_0^t v(\varsigma)\times$$
$$\times\left[\int_0^\varsigma\omega_0(\varsigma-\vartheta)v(\vartheta)d\vartheta-\theta(\varsigma)\right]d\varsigma\geq\eta_{01}^2, \quad (24)$$
$$\eta_{01}=const,\ \forall t>0,$$
where $\omega_0\left(\cdot\right)$ represents the pulse transient function of the generator for periodic signals with the transfer function $W(s)=\dfrac{1}{1-e^{-s\overline{T}}}$.

Let us synthesize $u_2(t)$ in the following combined form
$$u_2(t)=\gamma_{21}y_{ml}(t)\int_0^t y_{ml}(\varsigma)v(\varsigma)d\varsigma+$$
$$+\gamma_{22}y_{ml}^2(t)v(t), \quad (25)$$
$$\gamma_{21}=\tilde{\gamma}_{21}\tilde{b}^{-1},\ \gamma_{22}=\tilde{\gamma}_{22}\tilde{b}^{-1},$$
$$\tilde{\gamma}_{21},\tilde{\gamma}_{22}=const>0.$$

In this case we can estimate the second term from (22) as follows:
$$\eta_2(0,t)=$$
$$=\int_0^t\left(\tilde{b}u_2(\varsigma)v(\varsigma)+\chi y_{ml}(\varsigma)v(\varsigma)\right)d\varsigma=$$
$$=\tilde{\gamma}_{21}\int_0^t y_{ml}(\varsigma)\int_0^\varsigma y_{ml}(\vartheta)v(\vartheta)d\vartheta\varsigma+$$
$$+\tilde{\gamma}_{22}\int_0^t\left(y_{ml}(\varsigma)v(\varsigma)\right)^2d\varsigma+$$
$$+\chi\int_0^t y_{ml}(\varsigma)v(\varsigma)d\varsigma=$$
$$=\frac{\tilde{\gamma}_{21}}{2}\left(\int_0^t y_{ml}(\varsigma)v(\varsigma)d\varsigma\right)^2+ \quad (26)$$
$$+\tilde{\gamma}_{22}\int_0^t\left(y_{ml}(\varsigma)v(\varsigma)\right)^2d\varsigma+$$
$$+\chi\int_0^t y_{ml}(\varsigma)v(\varsigma)d\varsigma\geq$$
$$\geq\frac{\tilde{\gamma}_{21}}{2}\left(\int_0^t y_{ml}(\varsigma)v(\varsigma)d\varsigma\right)^2+$$
$$+\chi\int_0^t y_{ml}(\varsigma)v(\varsigma)d\varsigma\pm\frac{\chi^2}{2\tilde{\gamma}_{21}}\geq-\frac{\chi^2}{2\tilde{\gamma}_{21}}=-\eta_{02}^2,$$
$$\eta_{02}=const,\ \forall t>0.$$

The obtained estimates (24) and (26) ensure the validity of the integral inequality (21). At the same time, a technically feasible control law, ensuring achievement of both the auxiliary (14) and the main (13) control objectives, while considering (23) and (25), and accounting for the high speed of the *DCF* (6) (as per [Khalil, 2002]), due to the small value of T_0, will be explicitly formulated as follows:
$$u(t)=\left(u_1(t-\overline{T})+\gamma_1v(t)\right)+$$
$$+\gamma_{21}sat\left(y_{ml}(t)\right)\int_0^t sat\left(y_{ml}(\varsigma)\right)v(\varsigma)d\varsigma+ \quad (27)$$
$$+\gamma_{22}sat\left(y_{ml}^2(t)\right)v(t).$$

Therefore, if conditions (20) and (21) are satisfied, the equivalent system (19), (27), and consequently the modified system (8), (9) will be hyperstable within a specified range of uncertainty. If we choose the time constant T_0 to be small according to certain conditions, then the system (1)–(6), (12) with the synthesized control law (27) will be *L*-dissipative and maintain operability during structural ignition.

5 Simulation Example

To illustrate the effectiveness of the system (1)–(6), (12)–(27), let us consider the problem of compensating external harmonic disturbances in a vibration protected plant using hydraulic support (1)–(3). The initial data are as follows [Izrailovich and Grishaev, 2012]:

$$m_0 = 1;\ LA^2 = 0.5,\ \left(c_r + \frac{A^2}{E}\right) = 1,\\ \delta = 3,\ A = 0.1,\ S = 0.3. \tag{28}$$

We set the parameters of a piezoelectric vibration transducer (4) according to [Johnson et al., 1980] with the following values:

$$m = 0.2 \cdot 10^{-3},\ U_r v = 5,\ h_0 = 2 \cdot 10^{-5},\\ K_y = 6.34 \cdot 10^{-4},\ T_y = 3.55 \cdot 10^{-4},\\ \zeta_y = 15.28,\ K_f = 3.5,\\ T_f = 5.61 \cdot 10^{-3},\ \zeta_f = 0.707. \tag{29}$$

To ensure a stable balance position for the vibration protected plant, we define the system's command (reference) signal as a constant value

$$r(t) = r^* = 0, \tag{30}$$

and simulate the system with initial data (28) – (30) under varying amplitudes of the external disturbance

$$F(t) = B sin(\varphi t),\ B = const > 0,\ \varphi = 2. \tag{31}$$

During a series of computational experiments, we selected the numerical values for the parameters of the combined controller (27) and dynamic correctors (6), (15) as follows:

$$\gamma_1 = 15 \cdot 10^2,\ \gamma_{21} = 10^4,\ \gamma_{22} = 10^3,\\ T = 2 \cdot 10^{-2},\ T_0 = 7 \cdot 10^{-4},\ \overline{T} = 0.2. \tag{32}$$

The dynamic characteristics of the control system, as depicted in Fig. 2 and 3, indicate that the nonlinear repetitive control law (27), with specified parameters, maintains a stable equilibrium position of the vibration protected plant by compensating for harmonic disturbances of varying amplitudes through control signals applied to the active element of the hydraulic support.

It should be noted that as the amplitude of active disturbances increases, the main target condition (13) is achieved with good accuracy and speed. In particular, the control error in steady-state mode does not exceed 0.2% in all cases (initially, the error does not exceed 5.5%), and transient processes are completed within 7 seconds from the start of system operation.

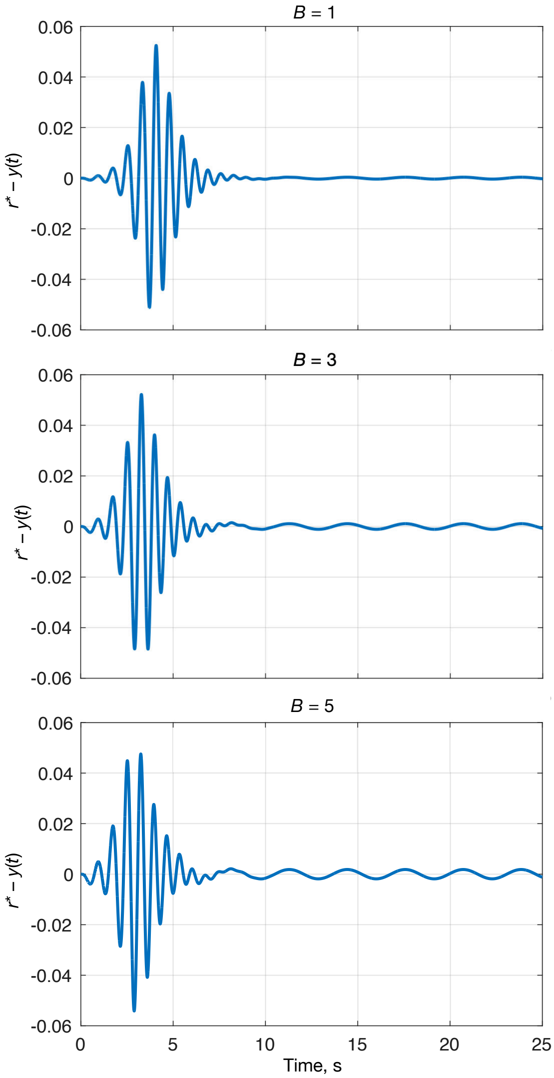

Figure 2. Control error at different values of the external disturbances amplitude.

Another important feature of the system is its ability to maintain operational efficiency and high performance indicators while compensating for disturbances with varying amplitudes (Fig. 4), frequencies (Fig. 5), or both parameters (Fig. 6).

6 Conclusion

A solution is proposed for damping forced vibrations in a vibration protection system using hydraulic support with active control. The author used a direct-conversion micromechanical accelerometer as a sensor to measure vibration displacements. The hyperstability criterion and a method for designing L-dissipative dynamic systems were used to synthesize the nonlinear feedback algorithms.

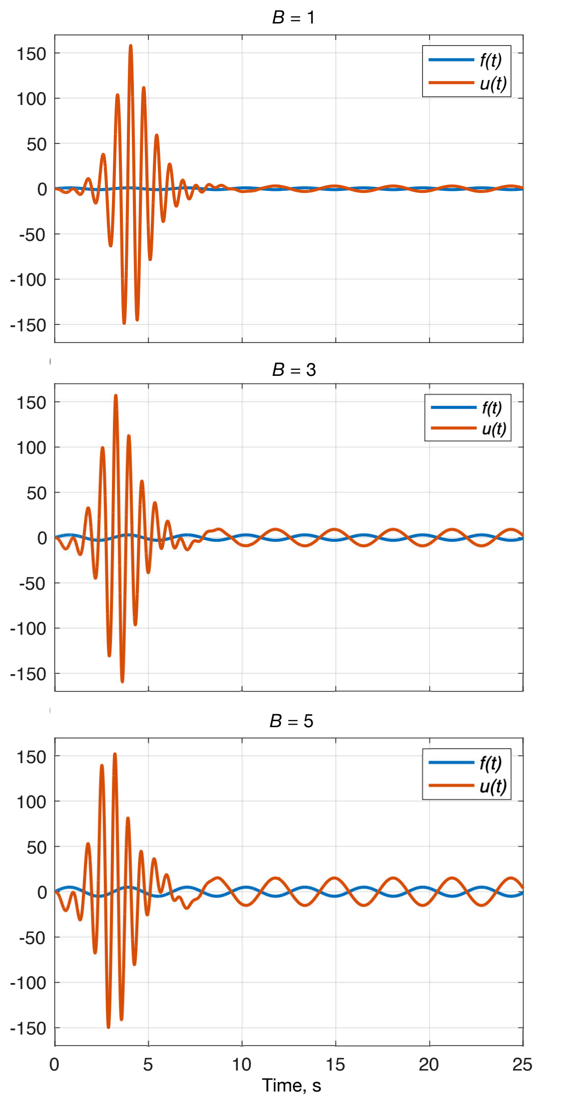

Figure 3. External perturbation with different amplitudes and respective control signals.

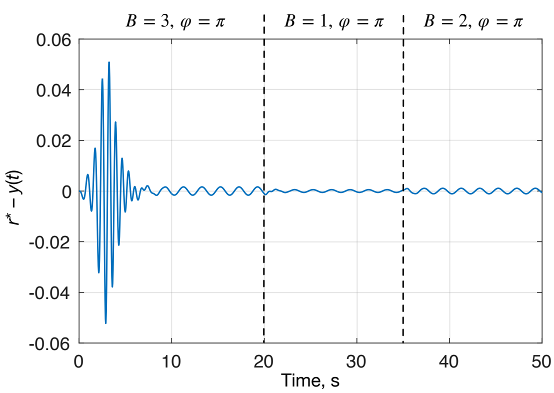

Figure 4. Control error at disturbance with changing amplitude.

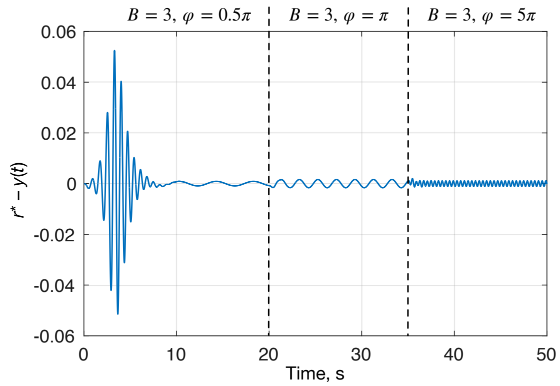

Figure 5. Control error at disturbance with changing frequency.

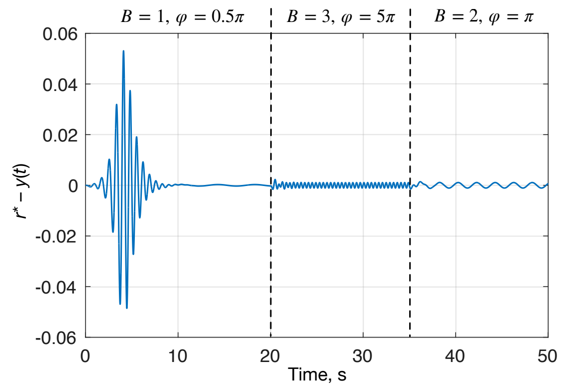

Figure 6. Control error at disturbance with both changing amplitude and frequency.

This approach allows us to design a combined vibration damping system. The quality of this system is demonstrated by the computational experiments that have been conducted.

Acknowledgements

This research was funded by the Ministry of science and higher education of the Russian Federation (project FEME-2024-0010);

References

Andrievsky, B. R. and Furtat, I. B. (2020a). Disturbance observers: Methods and applications. i. methods. *Automation and Remote Control*, **81** (9), pp. 1563–1610.

Andrievsky, B. R. and Furtat, I. B. (2020b). Disturbance observers: Methods and applications. ii. applications. *Automation and Remote Control*, **81** (10), pp. 1775–1818.

Bui, V. H. and Margun, A. A. (2022). Compensation of output external disturbances for a class of linear systems with control delay. *Scientific and Technical Journal of Information Technologies, Mechanics and Optics*, **22** (6), pp. 1072–1077.

Eremin, E. L. (2003). New type of parametric tuning algorithms of adaptive regulators for control systems of transitional T-periodic objects. *Information Science and Control Systems*, **2** (6), pp. 100–110.

Eremin, E. L., Nikiforova, L. V., and Shelenok, E. A. (2021). Nonlinear robust control of large-scale system with input saturation. *Cybernetics and Physics*, **10** (1), pp. 13–21.

Eremin, E. L., Nikiforova, L. V., Telichenko, D. A., and Shelenok, E. A. (2022). Adaptive control system for structurally undefined thermal power plant on set of functioning states. *Cybernetics and Physics*, **11** (2), pp. 67–73.

Eremin, E. L. and Shelenok, E. A. (2011). Output control with external harmonic noise compensation in priory uncertainty. *Bulletin of Pacific National University*, **1** (20), pp. 97–103 (in Russian).

Eremin, E. L. and Shelenok, E. A. (2023). Robust repetitive control for one class of non-affine undefined plants. *Sensors and Systems*, **2** (267), pp. 44–50 (in Russian).

Furtat, I. B. (2013). The compensating algorithm of unknown multi harmonic disturbances for plants with input delay. *Information and Control Systems*, **5** (66), pp. 19–25 (in Russian).

Izrailovich, M. Y. and Grishaev, A. A. (2012). *Active vibration damping of forced vibrations using parametric and force action (in Russian)*. URSS, Moscow.

Johnson, D. E., Johnson, J. R., and Moore, H. P. (1980). *A Handbook of Active Filters*. Prentice-Hall, New Jersey.

Khalil, H. K. (2002). *Nonlinear Systems*. Prentice Hall, New Jersey.

Nguyen, K. T., Vlasov, S. M., Pyrkin, A. A., and Skobeleva, A. V. (2022). Compensation of external disturbances for mimo systems with control delay. *Scientific and Technical Journal of Information Technologies, Mechanics and Optics*, **22** (4), pp. 666–673.

Pikina, G. A. and Pashchenko, F. F. (2021). Synthesis of third-order time-optimal control system for plants with extremum time response. *Automation and Remote Control*, **82** (12), pp. 2183–2191.

Popov, V. M. (1973). *Hyperstability of Control Systems*. Editura Academiei, Germany.

Quoc, D. V., Bobtsov, A. A., Nikolaev, N. A., and Pyrkin, A. A. (2021). Stabilization of a linear nonstationary system under conditions of delay and additive sinusoidal perturbation of the output. *Journal of Instrument Engineering*, **64** (2), pp. 97–103 (in Russian).

Shelenok, E. A. (2023). Hyperstability and L-dissipativity of the repeptitive control systems. *Information Science and Control Systems*, **4** (78), pp. 111–124 (in Russian).

Tsykunov, A. M. (2010). Indirect measurements-based compensation of disturbances at control of a linear plant. *Automation and Remote Control*, **71** (4), pp. 654–662.